

Laser-induced instabilities in liquid crystal cells with a photosensitive substrate

István Jánosy*, Katalin Fodor-Csorba, Anikó Vajda, and Tibor Tóth-Katona

Institute for Solid State Physics and Optics,

Wigner Research Centre for Physics, Hungarian Academy of Sciences,

H-1525 Budapest, P.O.Box 49, Hungary

(Dated: January 9, 2014)

Abstract

Liquid crystal layers sandwiched between a reference plate and a photosensitive substrate were investigated. We focused on the reverse geometry, where the cell was illuminated by a laser beam from the reference side. In planar cells instabilities occurred, static and dynamic ones, depending on the angle between the laser polarization and the director orientation on the reference plate. In cells where the molecules were aligned along the normal of the reference plate, dynamic pattern was observed at all angles of polarization. A simple model based on a photo-induced surface torque gives account of the findings. Light scattering studies revealed some basic properties of the instabilities.

PACS numbers: 61.30.-v, 61.30.Hn, 78.15.+e, 42.70.Df

* Corresponding author; janossy.istvan@wigner.mta.hu

I. INTRODUCTION

Optical reorientation of liquid crystals is known since decades [1]. In a typical experiment the initial director alignment in an oriented cell transforms into a new steady-state configuration under the influence of a light beam. There are, however, some cases when steady-state director pattern does not exist or it is not stable, even though the exciting beam is uniform both in time and space. Temporal as well as spatial instabilities were observed. As an example, temporal oscillations and spontaneous spatial pattern formation were found in Fabry-Perot resonators containing nematic liquid crystals [2, 3]. Irradiation of homeotropic films of liquid crystals with circularly polarized beam is known to cause undamped director precession [4–6]; in the same cells ordinarily polarized light beam with slightly oblique incidence induces chaotic director oscillations [7–9].

In the above-mentioned examples the source of director reorientation is the bulk torque, exerted by the electromagnetic field on the liquid crystal molecules. There is another mechanism of optical reorientation, namely photo-induced surface realignment of the director [10, 11]. This effect occurs when one of the plates of the liquid crystal cell is coated with a photosensitive material. Most often azo dyes are used as a coating substance, exhibiting *trans-cis* photoisomerization. When the cell is irradiated, the director on the photosensitive plate becomes oriented perpendicularly to the light polarization at the plate.

In a recent publication [12] we investigated cells, in which the liquid crystal was sandwiched between a "reference" plate, covered with a traditional, rubbed polyimide layer and a dye-coated plate. We found that instabilities occur in the liquid crystal film when the light beam enters the cell from the reference side (*reverse* geometry). In the experiment the polarized light from a microscope was used as the light source for excitation. The dominant instability was a static spatial pattern formation with a characteristic domain size of the order of a micrometer. At certain locations of the sample, however, dynamic instability was observed. In this structure the director oscillated or rotated continuously in a spatially inhomogeneous manner. The oscillation period was found to be proportional to the intensity of the illuminating light.

In the present communication further results are described in connection with this instability. We report on experiments where a monochromatic laser beam was applied for excitation instead of the white-light source used previously. In planar cells at ordinary input of

the exciting light (polarization perpendicular to the rubbing direction at the reference plate) the director configuration remained stable. At extraordinary input (polarization parallel to rubbing) static light-scattering occurred with a faint and broad conical maximum around a certain angle. When the angle between the light polarization and the rubbing direction was between o and e polarization, dynamic scattering developed. We present also results obtained in a cell where on the reference plate the liquid crystal molecules were aligned perpendicularly to the surface (so-called hybrid cell). In this type of cell dynamic behavior was observed at all angles of incident polarization. These experimental results are described in detail in Section II, while in Section III a simple model is presented, which provides an explanation of the findings. In addition, we studied the fluctuations of the scattered light (Section IV). In planar cells intermittency, i.e., the occurrence of relatively rare fluctuations of huge amplitudes were observed. The probability density function (PDF) of the scattered light intensity could be characterized by the generalized Fisher-Tippet-Gumbel distribution (gFTG) [13]. In the case of a hybrid cell neither gFTG nor Gaussian distributions did not provide a good description of the fluctuations; the PDF was between these two distribution functions.

II. BASIC OBSERVATIONS IN THE REVERSE GEOMETRY

The photosensitive plate was prepared in the same way as in our previous work [12] following the method worked out by Yi et al. [14]. The azo-dye utilized in the experiments was synthesized by coupling to methyl-red (3-aminopropyl) triethoxysilane, forming a derivatized methyl red (dMR). The dMR was chemisorbed on the glass surface in toluene solution. To prepare planar cells commercial, rubbed polyimide coated slides from E.H.C. Co (Japan) were applied as reference plates. $15 - 20\mu\text{m}$ thick cells have been filled with 4-cyano-4'-pentylbiphenyl (5CB), which is a room temperature nematic. Before and during the filling process the cell was illuminated with polarized light from a white LED source from the photosensitive side; the polarization direction was perpendicular to the rubbing direction. This procedure ensured good quality planar alignment of the cell. The preparation process of hybrid cells was similar to that of the planar one, except that the reference plate was coated with L- α -phosphatidylcholine (lecithin), which ensured homeotropic director orientation on that plate. Prior to and during filling the cell with the liquid crystal it was

irradiated again with polarized light. As a result, the initial director field was confined to the plane defined by the cell normal and the polarization direction of the irradiating light. The measurements were carried out at room temperature. The laser beam was focused to around $100\mu\text{m}$ spot size; its power was changed from a few μW to a few mW .

For excitation the beams from a green ($\lambda = 532\text{nm}$) and a blue ($\lambda = 457\text{nm}$) laser were used. The results were similar for the two wavelengths; in the paper data obtained with the green laser are presented. In the geometry, when the dye-coated plate was facing the illuminating beam (*direct* geometry), a simple reorientation process was observed. In this case the direction of the light polarization on the photosensitive substrate obviously coincides with the impinging laser polarization (on the contrary this is not the case for the reverse geometry. The director rotates on the dyed substrate toward the normal of the incident polarization, while on the reference plate it remains unchanged thereby inducing a twist in the cell [15].

The subject of the present paper is the investigation of the *reverse* geometry, i.e., the case when the cell is illuminated from the reference plate. First we describe the observations in planar cells; subsequently we discuss findings in hybrid cells.

In planar cells qualitatively different behaviors were observed depending on the angle between the rubbing direction and the polarization of the incoming light. We represent this angle by α , where $\alpha = 0$ denotes that the polarization is perpendicular to the rubbing direction. At $\alpha = 0^\circ$ the beam traversed the sample without any significant depolarization or scattering. This was as expected, since in this case the initial planar alignment on the photosensitive plate is stabilized by the illuminating beam. At $\alpha = 90^\circ$, i.e., when the incoming polarization was parallel to the director on the reference plate, static scattering took place. The scattered light exhibited a broad peak along a cone; for the green beam the aperture was about 20-30 degrees. This scattering obviously corresponded to the static domain structure, observed previously in a microscope [12]. From the aperture of the scattering cone one can estimate the domain size. It was found to be in the order of few micrometers, in good agreement with the findings in a microscope. At angles between 0° and 90° dynamic scattering arose in the form of random light intensity both in space and in time. In the scattering picture flashes of randomly oriented lines were observed as well. It was difficult to assign exact critical angles to transitions from non-scattering or static scattering regions to dynamically scattering ones; usually the interval $15^\circ < \alpha < 75^\circ$ belonged to the latter type

of instability. This mode of instability corresponds to the dynamical instability, observed at certain locations of the sample under a polarizing microscope at 90° [12]. However, in the present case, using a monochromatic light source, the turbulent director rotation was observed in the major part of the sample and at a certain range of the α values.

In order to characterize the dynamic nature of the instability, we recorded the temporal fluctuations of the scattered light S . A fiber optics was used to collect and to transmit to a photomultiplier a small part of the scattered light. The fiber was placed around the center of the halo observed at the static case (i.e. 15° away from the direct beam) and collected the scattered light from a cone with approximately 2° aperture. The sampling rate was around 5 Hz; the integration time of the intensity measurements was 20 ms. As an example, a trace observed at $\alpha = 45^\circ$ is presented in Fig. 1. As a comparison, we show also in Fig. 1 the corresponding curve for $\alpha = 90^\circ$, where no significant fluctuations were found. The detailed analysis of the scattered light fluctuations is presented in Section IV.

Observations for the direct geometry in the hybrid cells will be discussed elsewhere. In the reverse geometry dynamic instability was found in these cells, both using microscope light and laser beams. The instability was dynamic at arbitrary α angle, although it showed some dependence on this angle. The temporal fluctuations of the scattered light are displayed in Fig. 2 for three different values. The turbulence was less pronounced in the hybrid cells compared to that in planar ones: here less intense spikes were observed much more rarely than in the latter case.

III. MECHANISM OF THE INSTABILITIES

In the direct geometry the orientation of the liquid crystal molecules on the photosensitive plate is determined by the incoming polarization direction of the exciting light beam. In the reverse geometry the exciting radiation passes through the liquid crystal layer before impinging the photosensitive layer. While traversing the sample the state of polarization of the light wave can be modified due to the birefringence of the substance; the modification depends on the director pattern. In turn, the state of polarization at the photosensitive plate determines the surface director on this plate and thus the director distribution in the cell. Therefore, in the reverse geometry the photoalignment and the director field form a coupled system mutually influencing each other; as it will be demonstrated below, this coupling is

the reason behind the pattern formation.

The exact description of the dynamics of photoalignment and the corresponding director reorientation is a complex problem, which in our opinion is not yet fully solved. An approach was proposed by Kiselev et al [16], who associated photoalignment with a light intensity-dependent mean-field potential. In the present model we adopt this approach. In this paper we confine ourselves to monochromatic exciting light; the case of white light source will be analyzed elsewhere. We prefer to describe photoalignment through a light-induced surface torque on the director on the dyed plate, which can be derived from the mean-field potential, because it is straightforward to generalize it to elliptically polarized light. In the simplest form that is compatible with the symmetry of the problem it can be written in a similar form as the bulk optical torque, with the difference that it acts only at the photosensitive boundary:

$$\Gamma_{ph} = f \langle (\mathbf{n}_s \times \mathbf{E}_s) \mathbf{n}_s \cdot \mathbf{E}_s \rangle \quad (1)$$

where \mathbf{E}_s and \mathbf{n}_s are the electric field strength and the surface director on the photosensitive plate respectively; f is a positive constant and $\langle \rangle$ denotes time averaging over a period of oscillation of the electromagnetic wave. The above conjecture provides a qualitatively correct description of photo-alignment, including elliptically polarized exciting beams. For elliptic polarization the surface torque can be written as

$$\Gamma_{ph} = f E_o E_e \cos \Delta\Phi (\mathbf{n}_s \times \mathbf{e}_o)(\mathbf{n}_s \cdot \mathbf{e}_e) \quad (2)$$

where E_o and E_e are the amplitude of the ordinary and extraordinary components respectively; $\Delta\Phi$ is the phase difference between the e and o components; \mathbf{e}_o and \mathbf{e}_e are unit vectors along the ordinary and extraordinary polarization.

The next assumption is that the light propagates according to the Mauguin limit [17], i.e., the polarization ellipse follows adiabatically the rotation of the director within the sample in the presence of a twist deformation.

First we discuss planar cells. In the case of normal incidence the surface torque rotates the director within the photosensitive plate. When the input light on the reference plate is linearly polarized at an angle α in the planar cell the photoinduced surface torque given by Eq. (2) becomes

$$\Gamma_{ph} = f' I \sin 2\alpha \cos \Delta\Phi \quad (3)$$

with $\Delta\Phi = 2\pi(n_e - n_o)d/\lambda$. Here I is the intensity; n_e and n_o are the extraordinary and ordinary refractive indices, respectively; d and λ are the sample thickness and wavelength respectively; f' is a constant related to f .

Except of special cases, to be discussed below, the photoinduced torque is different from zero; therefore the director should rotate either clockwise or anti-clockwise, depending on the sign of $\cos\Delta\Phi$. Within the Mauguin limit the light polarization ellipse on the photosensitive plate is rotating together with the surface director, therefore the photoinduced torque remains constant in time. This torque is opposed by the surface elastic torque, which increases as the director rotation increases the twist in the cell. As shown, however, by experiments in the direct geometry [12], before a balance would be reached between the surface torques a disclination loop is formed in the sample, which reduces the twist. In this way the elastic torque is reduced, hence balance between torques is never established. This mechanism explains the observed dynamical behavior.

At $\alpha = 0^\circ$ and $\alpha = 90^\circ$ the photoinduced torque is zero. In the former case the director configuration is stable, while in the latter case it is unstable against small deviations from the perfect geometry. The second case show a certain analogy to the electric-field induced Freedericksz transition in a planar cell, where - in an ideal case - the transition is initiated by thermal fluctuations of the director. These fluctuations relieve the twofold degeneracy of the director rotation and lead to the formation of domains with opposite twists. The domains are separated by inversion walls, which are unstable, so finally, the domains merge and a uniform director rotation takes place. In our case, however, the situation is different from the electric-field induced Freedericksz transition in important aspects. First, static disorder of the alignment on the reference plate plays a much more significant role than thermal fluctuations as shown e.g. by Nespoulous et al. [18]. These authors studied SiO substrates and found a few degrees of spatial disorder in the alignment. The variation of the orientation on the reference plate results again in the formation of two types of domains, but this time the domains cannot easily merge because the walls separating them are attached to the substrate. In addition, the formation of a fine domain structure leads to the invalidation of the adiabatic light propagation; the light beam becomes depolarized on the photosensitive plate, which weakens its orienting strength, so that the elastic torque can balance the photoinduced one. These factors can results in the static spatial structure observed in the experiments.

We note that there is one more situation when the light-induced torque is zero: the case of $\cos \Delta\Phi = 0$, i.e., when an input beam with a linear polarization at $\alpha = 45^\circ$ becomes circularly polarized at the photosensitive layer. This occurs at special thicknesses of the sample obeying the relation

$$d = (m + \frac{1}{2}) \frac{\lambda}{2(n_e - n_o)} \quad (4)$$

where m is an integer. We plan to check in the future such situations [19].

In the case of hybrid cells, for the interval $0 < \alpha < 90^\circ$, the same argument can be used as for the planar case. Regarding the situation $\alpha = 0$ and $\alpha = 90^\circ$, we note that the disorder of orientation on the reference plate is not present, or at least it is much smaller than in the case of planar orientation. This may explain the fact that in these cells no static domains were found. Actually, there is an axial symmetry of the sample around the z axis, which would suggest that the scattering is independent from α . This argument is valid, however, only if there is no "easy axis", i.e., preferred director orientation on the photosensitive plate. Such a preferred axis, however, might be generated during the preparation of the cell; it may correspond to the normal direction to the light polarization used during the cell preparation. This can be one of the reasons of the observed deviations in the scattering strength for the three curves presented in Fig. 2.

To sum up, the reason of the dynamic instability is - similarly to the case of bulk instabilities [7–9] - the interplay of the extraordinary and ordinary components of the irradiating light beam. This effect works only with monochromatic light beams; the analysis of white light sources is still an open problem.

IV. ANALYSIS OF LIGHT SCATTERING

The description presented in the previous section showed that the uniform planar orientation must become unstable in the reverse geometry for $\alpha > 0$. Arguments were given to explain that why the distortion becomes static near $\alpha = 90^\circ$ and dynamic for $0 < \alpha < 90^\circ$. The above considerations, however, cannot elucidate the underlying nature of the instabilities, especially not that of the dynamic one. This task is beyond the scope of the current paper; we present nevertheless some empirical results in connection with light scattering. These findings, although they are preliminary, give some indications of the class the observed dynamic behavior belongs to.

The autocorrelation function of the scattered light intensity did not exhibit any structure, in particular it did not show oscillatory character. This fact seems to be in contrast with the occurrence of quasi-periodic oscillations that have been reported in [12] on the basis of observations in a polarizing microscope. Considering the results shown in Fig.3 of Ref. [12], the oscillations at the given light intensity could be expected to occur around 1.5Hz. However, in [12] a much larger spot was illuminated than in the laser experiments (mm -s versus $100m\mu$ -s). In the former case - after some time - a quasi-periodic structure was organized, which seems to be absent in the latter one. We note that the same light-scattering experiment was repeated with a much higher sampling rate (100 Hz); the result was similar as with the low sampling rate.

We investigated also the probability density function (PDF) of the scattered light. As it can be seen from Fig. 1, in a planar cell the scattered light occasionally increased sharply. These spikes could be followed by eye also in the scattering picture; they corresponded to flashes of randomly oriented lines, as mentioned in Sec. II. Such intermittent behavior is well-known to occur in a great number of disparate systems e.g., in turbulent flow [20–22], in Danube water level fluctuations [23, 24], in the simulations of the 2D X-Y model at criticality [13, 21, 25], or in electroconvection of liquid crystals [26]. In all these systems the probability density function of the measured quantities follows the generalized Fisher-Tippett-Gumbel (gFTG) distribution [13] which has a form of

$$\pi(S)\sigma_S = K \exp[b(x - c) - e^{b(x-c)}]^a \quad (5)$$

where $K = 2.14$, $b = 0.938$, $c = 0.374$, $a = \pi/2$, and

$$x = (S - \langle S \rangle) / \sigma_S \quad (6)$$

In our case: $\pi(S)$ - PDF of the fluctuations of the light intensity scattered into the observed area, S ; $\langle S \rangle$ - the mean value of the scattered light intensity; σ_S - the standard deviation of the S fluctuations. Note that gFTG distribution presented by Eq. (5) has a universal form, without any fit parameter. The gFTG distribution is substantially skewed with one tail described by an exponential decay which is considered to be due to fluctuations having a length scale comparable to the system size [21, 22, 27].

In Fig. 3 we present the normalized PDFs deduced from our measurements with $\alpha = 45^\circ$ and $\alpha = 90^\circ$ of the incoming light. The solid lines correspond to the Gaussian and

gFTG distributions (without a fit parameter) as denoted in the legend. Clearly, in case of $\alpha = 90^\circ$ the central limit theorem holds. In this geometry the source of the fluctuations is mainly the laser and the dark current of the photomultiplier; the intensity fluctuations have Gaussian distribution suggesting that they arise from many uncorrelated contributions. On the contrary, for $\alpha = 45^\circ$ the PDF of the fluctuations follow the gFTG distribution. This is an indication of an essential difference between the lights scattered from the static and dynamic domains.

The fluctuations of scattered light have also been analyzed for a wide range (of almost three orders of magnitude) of input powers P . Fig. 4 shows the temporal dependence of the scattered light intensity in the range of input powers from $P = 12\mu\text{W}$ to $P = 4.2\text{mW}$ for $\alpha = 45^\circ$ of the incoming light. Qualitatively, the temporal dependencies seem self-similar. As a quantitative measure of the self-similarity we have plotted the normalized PDFs of these fluctuations in Fig. 5. As one can see the fluctuations follow satisfactorily the gFTG distribution over the whole range of the input power investigated.

In Sec. III it was pointed out that the dynamic instability is related to the continuous generation/annihilation of disclination loops. We assert that the spikes observed in the case of planar cells arise from disclination lines, passing through the area illuminated by the exciting light beam. In the restricted irradiated area spikes are probably due to individual disclination loops. This circumstance is deduced from the observation by eye, where the scattered lines are seen individually.

In a recent paper it has been argued that the asymmetry of the energy distribution is driven by a finite energy flux crossing the system from injection to dissipative scales [28]. In the same time, as it has been pointed out, a comparison with a real experimental system (such as the turbulent flow) is not directly feasible, due to a number of simplifications in the phenomenological approach [28]. Despite of that, some comments on the experiments can be made in this regard. In our case the disturbed area in the sample for a focused beam is larger than the laser spot due to long-range elastic interactions in the nematic (just as in the case of static optical Freedericksz transition with finite beam size, where the director distortion has an essentially longer range than the laser diameter [29, 30]). Therefore, we assert that disclination loops are nucleated in a larger area than the scattered one. However, if one suppose that dissipative scales are connected to the deformation zone in the director field around the disclination lines only, then the idea of Bertin and Holdsworth [28] may be

relevant to our system. Future investigations of the PDF dependence on the laser spot size may help to clarify this question.

As mentioned in Section 2, for hybrid cells the fluctuations are less pronounced, spikes are basically absent. The PDFs of the fluctuations for this case are presented in Fig. 6. The data for all polarization direction collapse into one "intermediate" PDF (in spite of the intensity differences shown in Fig. 2) which deviates both from the Gaussian and from the gFTG distributions, and represents a midway distribution between them. In the case of hybrid cells the undamped rotation of the director can take place in a much smoother way than in the planar case; disclination loops are only generated in the vicinity of the border of illuminated area. This fact could explain the scarcity of spikes for the hybrid cell. The situation is analogous to the distribution of injected power fluctuations in electroconvection [21]. In those measurements for the unconfined geometry, a departure from the normal distribution towards the gFTG one has been observed above the anisotropic to isotropic turbulence, when the density of the disclination loops is abruptly increased.

In conclusion, the observed light scattering from chaotic director movement is analogous to observations of turbulence in many different systems. Further work is needed to elucidate the similarities and differences in the details.

V. CONCLUSIONS

In this paper the previous studies of light-induced instabilities in cells with a photosensitive substrate were extended to the case of laser illumination. We found that using a monochromatic light source dynamic instability can be generated in planar cells by choosing the polarization angle of the exciting beam in a proper range. In hybrid cells we observed dynamic instability at arbitrary angle of polarization, although the director turbulence was less pronounced in this case than in the former one. These observations were confirmed by light scattering studies as well. A simple model was presented, which qualitatively explains the onset of the instabilities.

It is remarkable that a seemingly trivial extension of the standard photoalignment experiments, namely reversing the illumination direction of the exciting light, leads to the highly nontrivial phenomena described in the paper. As we pointed out, the reason for pattern formation is that in the reverse geometry the photoalignment and the director reorienta-

tion processes are coupled together and their mutual interaction gives rise to the observed behavior of liquid crystal cells.

Acknowledgments

The work was supported by the Hungarian Research Fund OTKA K81250.

-
- [1] L. Marrucci, Y.R. Shen, Nonlinear optics of liquid crystals, in *The optics of thermotropic liquid crystals*, eds. R. Sambles and S. Elston (Taylor and Francis, London, 1998).
 - [2] M. M. Cheung, S. D. Durbin, and Y. R. Shen, Opt. Lett. **8**, 39, (1983).
 - [3]] M. Kreuzer, W. Balzer, and T. Tschudi, Appl.Opt. **29**, 579 (1990).
 - [4] E. Santamato, B. Daino, M. Romagnoli, M. Settembre, and Y. R. Shen, Phys. Rev. Lett. **57**, 2423 (1986).
 - [5] A.S. Zolot'ko and A. P. Sukhorukov, JETP Lett. **52**, 62 (1990).
 - [6] E. Brasselet, T. V. Galstian, L. J. Dubé, D.O. Krimer, and L. Kramer, J. Opt. Soc. Am. B **22**, 1671 (2005).
 - [7] A.S. Zolotko, V.F. Kitaeva, N. Kroo, N.N. Sobolev, A.P. Sukhorukov, V.A. Troshkin, and L. Csillag Sov. Phys. JETP **60**, 488 (1984).
 - [8] G. Cipparrone, V. Carbone, C. Versace, C. Umeton, R. Bartolino, and F. Simoni, Phys. Rev. E **47**, 3741 (1993).
 - [9] E. Brasselet and L. J. Dubé, Phys. Rev. E **73**, 021704 (2006).
 - [10] W.M. Gibbons, P.J. Shannon, S.T. Sun, and B.J. Swetlin Nature **351**, 49(1991).
 - [11] K. Ichimura, Chem. Rev. **100**, 1847 (2000).
 - [12] I. Jánossy, K. Fodor-Csorba, A. Vajda, and L. Palomares, Appl. Phys. Lett. **99**, 111103 (2011).
 - [13] S.T. Bramwell, K. Christensen, J.-Y.Fortin, P. C.W. Holdsworth, H. J. Jensen, S. Lise, J.M. López, M. Nicodemi, J.-F. Pinton, and M. Sellitto, Phys. Rev. Lett. **84**, 3744 (2000).
 - [14] Y. Yi, M. J. Farrow, E. Korblova, D. M. Walba, and E. Furtak, Langmuir **25**, 997 (2009).
 - [15] This photoalignment process normally worked for about a month, afterwards it could not be observed. A possible reason is that the azo layer was gradually dissolved in the liquid crystal layer.

- [16] A. D. Kiselev, V. G. Chigrinov, and H.-S. Kwok, Phys. Rev. E **80**, 011706 (2009).
- [17] M.C. Mauguin, Bull. Soc. Fr. Mineral. **34**, 71 (1911); H. de Vries, Acta Cryst. **4**, 219 (1951).
- [18] M. Nespoulous, Ch. Blanc, and M. Nobili, Phys. Rev. Lett. **104**, 097801 (2010).
- [19] Since the submission of the paper, we carried out experiments on wedge-like cells. We found that dynamic instabilities do not take place at positions where $\cos \Delta\Phi = 0$, in agreement with the model presented here. Details will be published in the Proceedings of the *Optics of Liquid Crystal* conference (Honolulu, 2013).
- [20] O. Cadot, S. Douady, and Y. Couder, Phys. Fluids **7**, 630 (1995).
- [21] S.T. Bramwell, P.C.W. Holdsworth, and J.-F. Pinton, Nature (London) **396**, 552 (1998).
- [22] J.-F. Pinton, P.C.W. Holdsworth, and R. Labbé, Phys. Rev. E **60**, R2452 (1999).
- [23] I. Jánosi and J.A.C. Gallas, Physica A **271**, 448 (1999).
- [24] S.T. Bramwell, T. Fennell, P.C.W. Holdsworth, and B. Portelli, Europhys. Lett. **57**, 310 (2002).
- [25] S. Aumaitre, S. Fauve, S. McNamara, and P. Poggi, Eur. Phys. J. B **19**, 449 (2001).
- [26] T. Tóth-Katona and J.T. Gleeson, Phys. Rev. Lett. **91**, 264501 (2003).
- [27] B. Portelli, P.C.W. Holdsworth, and J.-F. Pinton, Phys. Rev. Lett. **90**, 104501 (2003).
- [28] E. Bertin and P.C.W. Holdsworth, Europhys. Lett. **102**, 50004 (2013).
- [29] B. Ya. Zeldovich, N.V. Tabiryan, and Yu.S. Chilingarian, JETP **54**, 32 (1981).
- [30] L. Csillag, I. Jánossy, V.F. Kitaeva, N. Kroó, and N.N. Sobolev, Mol. Cryst. Liq. Cryst. **84**, 125 (1982).

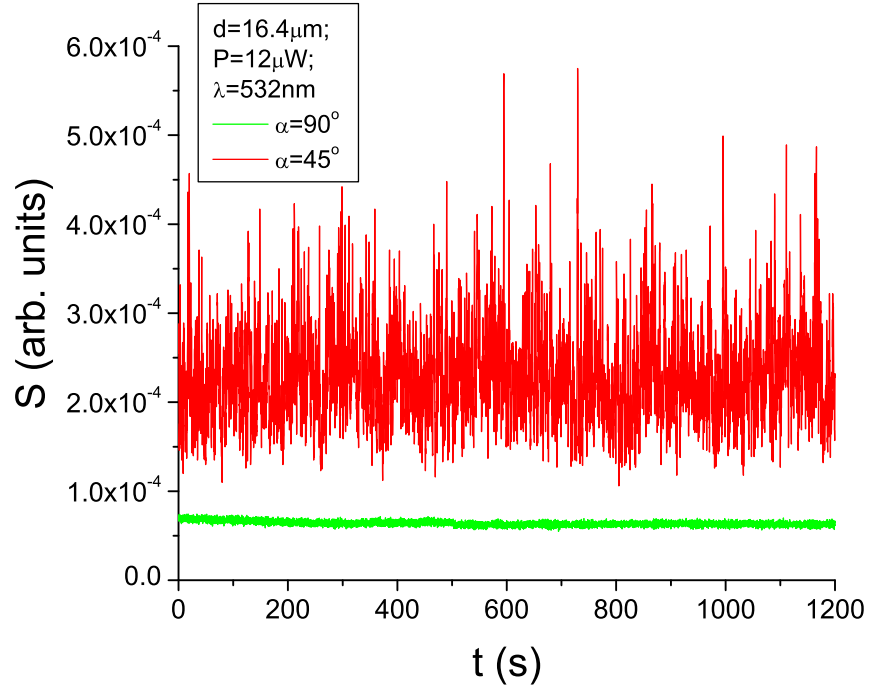


FIG. 1: (Color online) Temporal dependence of the scattered light intensity for the polarizations $\alpha = 90^\circ$ and $\alpha = 45^\circ$ of the incoming light in the reverse geometry, measured in a planar cell.

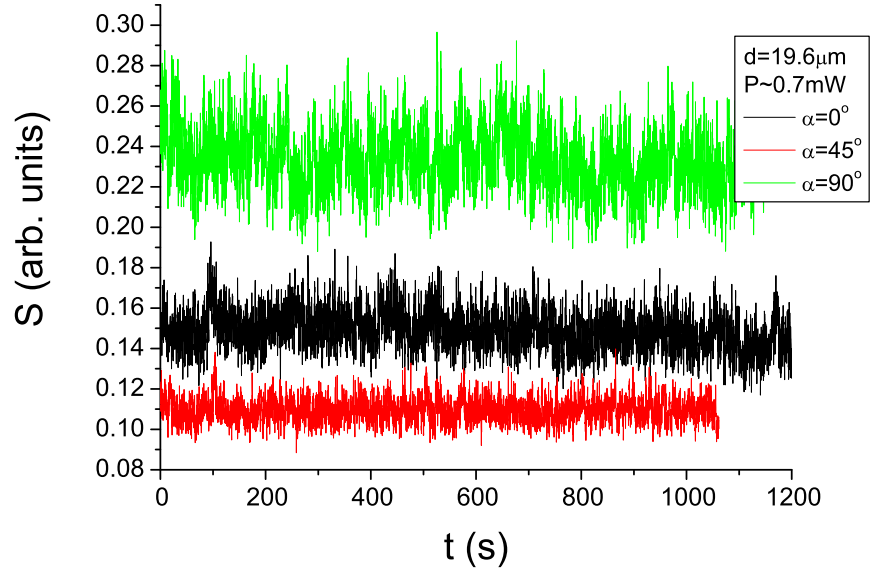


FIG. 2: (Color online) Temporal dependence of the scattered light intensity for different polarizations at the power of about 0.7mW of the incoming light in the reverse geometry measured in a hybrid cell.

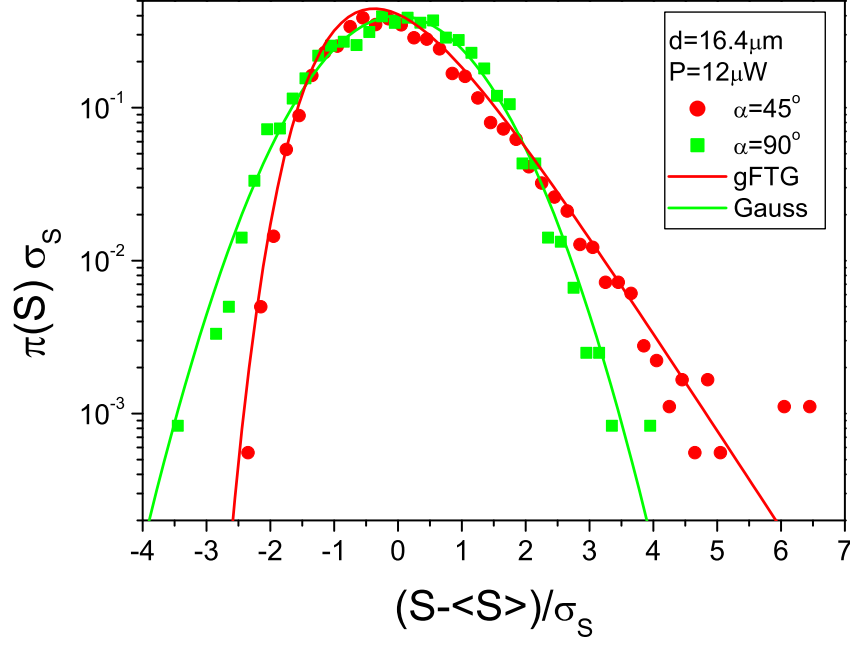


FIG. 3: (Color online) Normalized probability density function of the scattered intensity fluctuations detected in a planar cell for the polarizations $\alpha = 90^\circ$ and $\alpha = 45^\circ$ of the incoming light in the reverse geometry. Solid lines represent Gaussian and gFTG distributions without fit parameters as denoted in the legend.

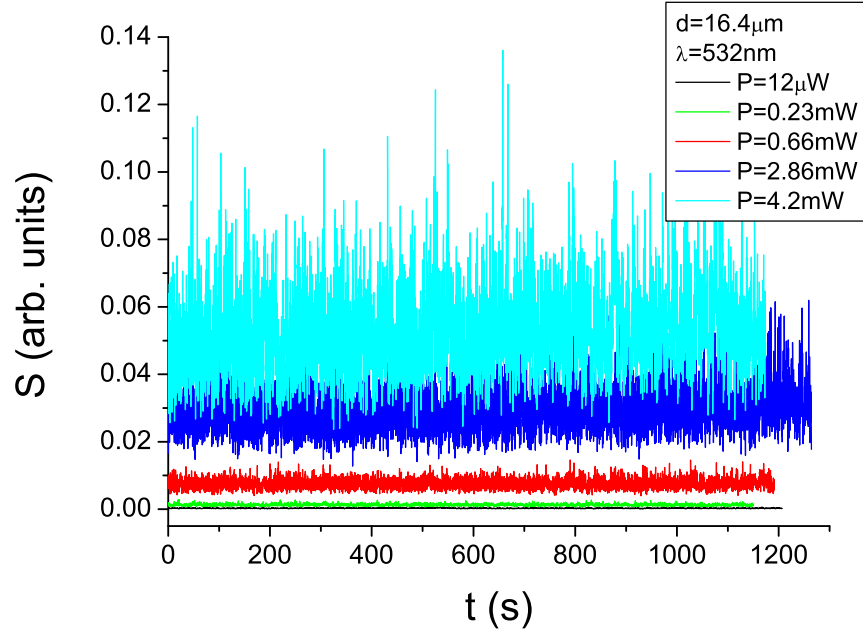


FIG. 4: (Color online) Temporal dependence of the intensity fluctuations measured in a planar cell for the polarization $\alpha = 45^\circ$ at different powers of the incoming light in the reverse geometry.

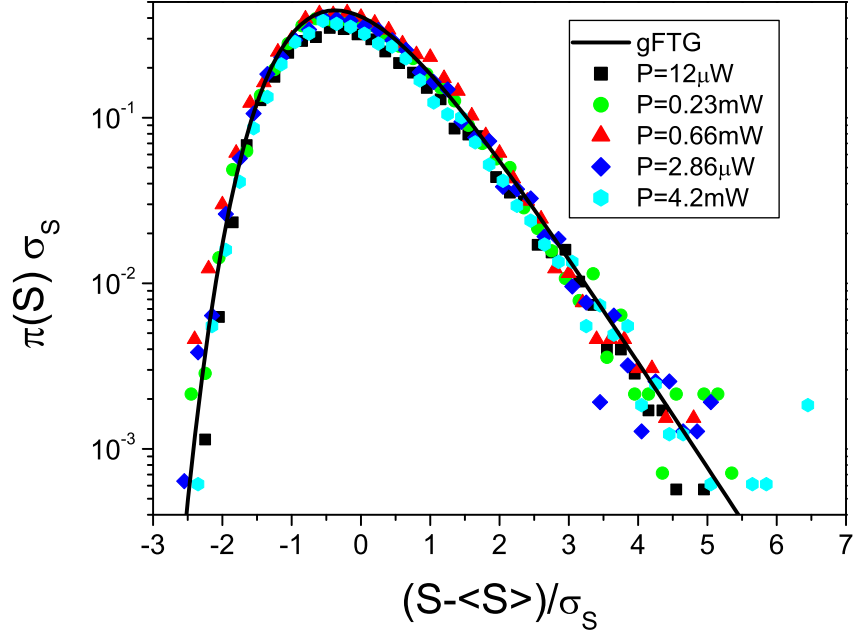


FIG. 5: (Color online) Normalized probability density function of the intensity fluctuations detected in a planar cell for the polarization $\alpha = 45^\circ$ at different powers of the incoming light (as denoted in the legend) in the reverse geometry. The solid line represents the gFTG distribution without any fit parameter.

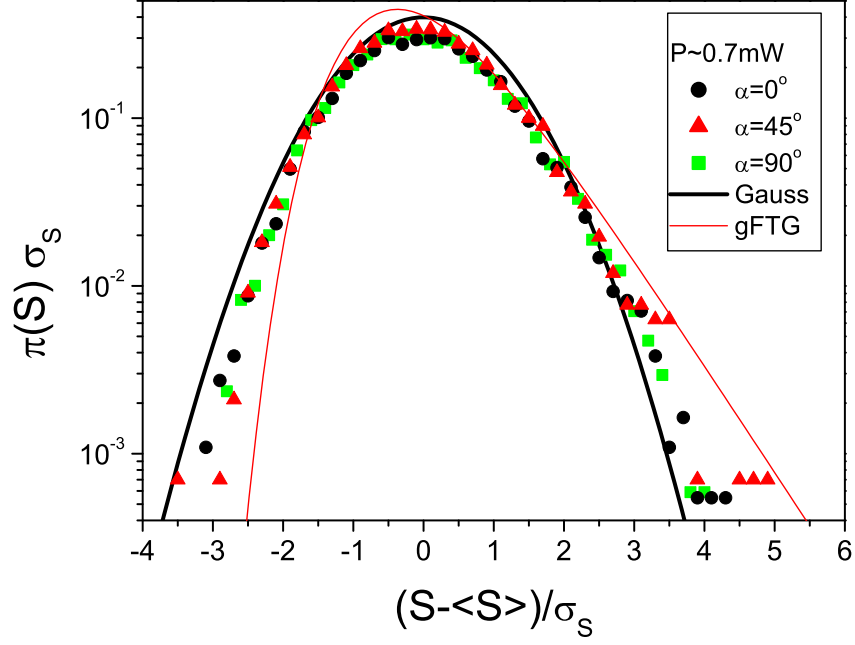


FIG. 6: (Color online) Normalized probability density function of the intensity fluctuations detected in a hybrid cell for the power $P \sim 0.7$ mW of the incoming light at different polarization directions (as denoted in the legend) in the reverse geometry. The solid lines represent the Gaussian and the gFTG distribution without any fit parameter.